European Journal of Technique

journal homepage: https://dergipark.org.tr/en/pub/ejt

Vol.13, No.2, 2023

Research Article

The SMaRt: Design, implementation, and experiment

Ahmet TOP[1*], Gökhan GÜNGÖR[2], Muammer GÖKBULUT[3]

[1*]Fırat University, Technology Faculty, Electrical Engineering Department, Elazığ, Turkey. (e-mail: atop@firat.edu.tr).
[2] Karabük University, Engineering Faculty, Mechatronics Engineering, Karabük, Turkey. (e-mail: gokhangungor@karabuk.edu.tr).
[3] Fırat University, Technology Faculty, Electrical Engineering Department, Elazığ, Turkey. (e-mail: mgokbulut@firat.edu.tr).

ARTICLE INFO

Received: Aug., 10. 2023
Revised: Sep., 26. 2023
Accepted: Dec, 25. 2023

Keywords:
Mobile robot control
Motion planning
İmage processing
Teaching
Education

Corresponding author: *Ahmet TOP*

ISSN: *2536-5010* | e-ISSN: *2536-5134*

DOI: https://doi.org/10.36222/ejt.1340895

ABSTRACT

Mobile robots, for teaching and research activities, have an important place in all education levels, from higher to primary education. They provide a malleable platform to meet research and teaching needs in various engineering and science fields, such as mechanics, electronics, software, biology, and psychology. However, their high cost and the difficulty of learning the user interface and programming tools prevent the widespread use of mobile robots. In this study, we develop an affordable, symmetric, modular, interactive, human-aware, autonomous, and four-wheel-driven mobile robot to boost the quality of education and research. The proposed mobile system is fully customizable with open hardware, software, and data to meet the unique demands and specifications of teaching and research. The developed mobile robot has been successfully operated for education and research purposes.

1. INTRODUCTION

Today, robots are used extensively in industry and provide significant benefits, and their impact becomes more visible as their usage increases in daily life [1]. They have great potential in teaching and research activities [2]. Robotics systems provide learners and researchers with education and research environments allowing them to incorporate ideas within science, technology, engineering, and mathematics (STEM) [3]. The basic concept of robot usage in teaching and research fields is to improve one's soft skills and integrate technical knowledge with practical experience, enhancing interest, engagement, creativity, motivation, and accomplishments in various STEM fields [4]. Such systems have a wide range of usage from entry-level educational institutions [5] to universities [6]; they are also used for non-technical support, for instance, for those with learning disabilities [7].

Many teaching strategies have been studied, and the methods are mainly designed to be cost-effective and time-efficient [8]. The reader is addressed to [9] for more details regarding learning techniques and strategies. There is a growing interest in interactive learning methods, and emerging technologies have been prevalent and made learning easy to apprehend [10]. Although they are more costly than classical learning methods, such systems ensure that students are instructed using state-of-the-art technology, and researchers can have experience with advanced applications [11].

Several robot platforms, such as manipulators and mobile robots, have been developed for educational and research purposes [12,13]. However, price, functionality, compactness, and user-friendly interface are important to embark on the robot selection process before making the final decision. Ceccarelli [14] introduces some low-cost robots and discusses how the robots are appropriately adapted for research and teaching activities. Piepmeier et al. [15] discuss robotics education principles and how they enhance teaching quality with robots.

The works related to the manipulators are given in [16– 19]. Those works related to robot manipulators cover student experiences with kinematic analysis and computer vision. Humanoid robots such as the NAO [20] are used in numerous institutions, allowing one to gain multi-disciplinary skills and develop content with seamless cases. However, they are pricey for teaching and research institutions have a limited allocation. Although their usages are feasible for graduate studies, they are expensive for undergraduate studies considering a class size of more than 30 students. For instance, the NAO AI edition costs $14990.

Mobile robots offer a cost-effective solution to explore these new learning and research methods [21–23]. There are several mobile robots presented for teaching and research activities. In order to integrate robotics research with undergraduate education, a university team developed a mobile robot called Rusty [24]. E-puck [25], designed at a low cost $850, is a mobile robot platform operated as a swarm robot [26-28] due to its small size and modular structure. The E-puck

consists of four parts: the main body, the led ring, and two wheels.

The LEGO Mindstorms platforms allowing flexibility to construct various robot configurations are utilized in numerous educational institutions for basic and advanced classes [29–31]. Still, they have hardware and software limitations for research activities. The price of the LEGO Mindstorms Core robot kit is around $850. Do [32] presents a mobile robot to apply image processing algorithms for multi-objective robot vision projects. For secondary education, the Scribbler robot, designed by Parallax [33], costs $229. The Scribbler is sufficient for teaching activities for secondary education but has weak hardware equipment to fulfill the undergraduate and graduate-level course requirements.

The Quanser QBot 3 [34] is an autonomous two-wheel drop and cliff sensor, 3-axis gyroscope) and a Red-Green Blue-Depth (RGB-D) camera. This robotic platform is mainly designed for undergraduate teaching and advanced graduate-level research applications such as machine learning and computer vision. The Quanser QBot 3 deploys applications through Simulink, Python, and the Robot Operating System (ROS). Developed by Adept Mobile Robots, Pioneer 3-DX is also one of the mobile robots for research and teaching activities [35]. The microcontroller on the robot has firmware called ARCOS. There also exists its three-dimensional model in the Gazebo simulation environment. There are eight ultrasonic sensors, encoders, and microcontrollers on the robot, and sensors such as laser, microphone, and gyroscope are mounted when required. The robot's production currently has been discontinued.

Another mobile robot developed for educational and research purposes is Turtlebot 2, one of the most popular open-source commercial educational robots [36]. Application for any teaching and research activity is executed with ROS, OpenCV, and Point Cloud Library (PCL). Its list price is about $1450. Studies by Gritti et al. [37], Wu et al. [38], and Barber et al. [39] are examples of works operated on this robot. The upgraded version of the Turtlebot 2 is named Turtlebot 3 [40]. It has two released versions: Burger and Waffle. The Waffle robot is larger and has extra sensors pushing it more expensive than the Burger. The Burger and the Waffle robot prices are approximately $660 and $1660, which are not high-cost robot platforms for higher education and research activities. The Turtlebot platform provides robust open-source software with the ROS environment. It has a modular plate so the user can modify the robot's shape. The hardware mounting kit consists of two dynamixel motors, a Light Detection and Ranging (LIDAR) sensor, a camera, and a single board computer with Intel Joule 570x. Amsters and Slaets [41] investigate how they successfully employ the Turtlebot 3 in graduate-level classes.

The latest version of the TurtleBot, called Turtlebot 4 [42] offers a Raspberry Pi 4 card running ROS 2, a spatial AI stereo camera, a LIDAR, an optical floor tracking sensor, and infrared and slip detection sensors. Turtlebot 4 costs $1850 for the standard model. All the TurtleBots and the Quanser QBots are powerful open-source platforms for learning and research development, but they are not fully operational when they work in outdoor activities. Such robotic systems mainly employ indoor laboratories, limiting operating real-time outdoor scenarios.

The **S**ymmetric **M**odul**a**r **R**obo**t** (SMaRt) provides services in both structured and unstructured environments. Outdoor robot experiences are significant to the researchers working in the field of robotics to handle many challenges regarding different working environments. The developed robot allows the implementation of advanced applications such as path-planning, mapping, and real-time image processing. For example, one can apply and test any algorithm to the SMaRt under different weather conditions. Moreover, the robot works in the military, service, and health research fields due to its durable, symmetric, and shock-reducing spring structure.

This paper presents the SMaRt design and its capabilities for both teaching and research activities. The developed robot is an affordable, modular, interactive, human-aware, autonomous, and four-wheel-driven system that is worked in structured and unstructured environments (see Figure 1), and it only costs $ 1521$. Thus, the students and researchers can operate many industrial and real-time scenarios with the developed robot; therefore, they can quickly adapt such experiences to real-time work and improve their debugging skills experimentally.

2. THE SMaRt MECHANICAL DESIGN

The mechanical design procedure of a mobile robot may not seem to be the central focus of the recent robotics work trend; however, it impacts the robot's reliability, durability, aesthetics, robustness, and safety. Adjusting the robot's weight-power ratio for energy efficiency with a low cost is one of the primary considerations of the mechanical design procedure; therefore, an ideal balance between robot dimensions and motor power is required to achieve a good design. Moreover, during the design procedure, it is important to consider how the robot will move, whether it will work around people, what kind of tasks it will perform, and how it will evaluate the environment.

In this study, the mechanical and electronic components of the mobile robot are positioned on the static platform as balanced as possible. There are two essential parameters to be considered in terms of weight properties during the robot design: the total mass/the weight per wheel and the center of the total mass. Each wheel is treated as the vertex of a polygon, and a support polygon is established with four wheels. Moreover, having a center of mass as far as away from the edges of the support polygon makes the system more stable in tipping over. Therefore, the components are placed where the center points further away from the edges, and the mass is concentrated near the center. This study uses the four-wheel-driven system to increase the support polygon's size, improving the robot's maneuverability and enacting its usage in indoor and outdoor applications. The SMaRt has wheels with wide, compliant tires suitable for traversal of mixed terrain with minor obstacles.

Four main components shape the backbone of the system: mechanical parts, a static platform, wheels, and motor holders. The robot's weight also plays a crucial role in the robot's mobility. It is a fact that the torque required to drive the robot will exponentially rise when an increase in the robot's weight is required. Lightweight metals are used to lighten the weight of the mechanical platform. Therefore, the design of the mobile robot with controllers and power supply is minimized for weight reduction to increase their moving abilities. The platform is constructed of 2-mm thick solid sheet metal, and holes are drilled to reduce the system's overall weight, allow ventilation, and include other optional add-ons. The material used for the chassis is determined to meet the structural needs of the potential robot operations. The total weight of the robot prototype is 9396 grams. The robot calculations during the design procedure are made with 10 kg weight under 10- degree road slope conditions. The actuator section gives details

regarding the required power to drive the robot. The mobile robot's mechanical design and its off-the-shelf component placements are shown in Figs. 1a and 1b, respectively.

(a)

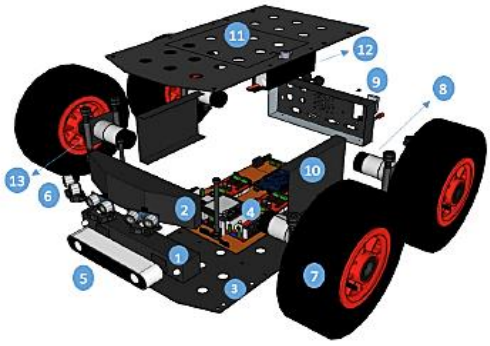

(b)

1:Camera module
2:Sensor module
3:Subframe
4:Electronic circuit board
5:Camera
6:Sensors
7:Wheel
8:Motor
9:Rear panel
10:Side panel
11:Upper frame
12:Battery
13:Motor holder

Figure 1. (a) Views of the SMaRt from different angles and (b) the off-the-shelf 3D model rendered in SketchUp.

The wheels are inflatable and have a diameter of 21 cm and a width of 6 cm, providing the robot system with 5.5 cm ground clearance distancing from the platform to the wheel. The chassis length, height, and width are 40 cm, 10 cm, and 22.2 cm, respectively. The platform also has an offset of 3.5 cm from the robot chassis in both the up and down directions due to the wheel size being longer than the platform size in terms of height to protect against possible chassis crushing. Moreover, the robot ground clearance dimensions are kept similar to either side of the robot to construct the robot symmetric. So, the robot can sense the turning upside down with an Inertial Measurement Unit (IMU) and continue to work due to its symmetric dimensions even when the flipping over occurs.

The robot fix platform is easily attached and removed from the motor shafts with screws. Sensors and removable attachments are placed on the front. On the back side of the robot, there are connectors such as micro-universal serial bus (micro-USB), USB, and High-Definition Multimedia Interface (HDMI). Moreover, light-emitting diodes (LEDs), buttons, battery indicator, Light Dependent Resistor (LDR) module, and fan are mounted to the back panel with the robot's external electrical connections (see Fig. 1a). As seen in Fig. 2, the motor and motor holders are fixed to the body with nuts. The springs, located between the body and the engine holder in the lower and upper parts, act as shock absorbents and reduce external disturbances. Therefore, the suspension system allows the robot to work in challenging terrain operations. Since the platform provides modularity, other add-ons are utilized for changing the driving system configuration if needed.

Moreover, mechanical power generated from the actuators is supervised according to a regulation defining robots having less than 80W mechanical power as safe since the developed robot is used for indoor and outdoor applications without being separated by a fence. The SMaRt, with a motor power of less than 80W, can be operated without installing a fence; therefore, it allows the robot to interact with humans, leading to the utilization of the SMaRt in many fields.

Figure 2. The drive system is used in the mobile platform.

3. THE SMaRt HARDWARE FEATURES

This paper considers a fully open hardware approach to improving the quality of education and research, which sustains innovation and enables the system to be used more efficiently. In addition, open-source hardware can significantly reduce research and education costs and contribute to collaborative science. The hardware architecture of SMaRt is shown in Fig. 3.

1:Boost converter
2:3.3 V Buck converter
3:Motor driver
4:Bluetooth module
5:Actuator
6:Humidity and temperature sensor
7:IMU
8:Lidar
9:Ultrasonic sensor
10:Infrared sensor
11:Camera
12:LattePanda
13:LDR Module
14:Arduino Due
15:Battery
16:5 V Buck converter
17:Battery display
18:Fan
19:Battery charger connector

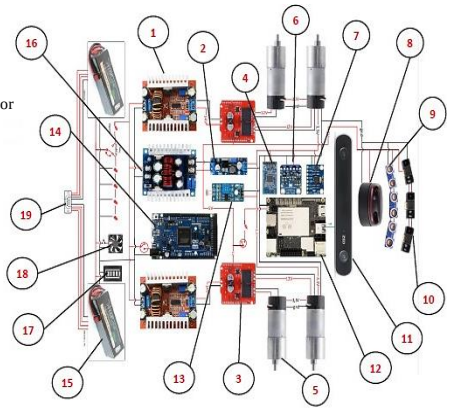

Figure 3. Hardware architecture of the SMaRt.

Multiple sensor devices can be used separately or together depending on the robot's operations, allowing many different robot tasks. The robot is modular, so the sensors can be placed on the robot at any time and easily included on the circuit board (see Fig. 4). The hardware architecture will be described in three parts: control boards, motors and drivers, and sensors.

1) Control Boards: This study uses two development boards, Arduino Due and LattePanda. While the Arduino controls the motor and peripherals as a central controller, the LattePanda is used as an auxiliary controller for the front camera, LIDAR, and sensors.

The main reason for using the Arduino Due is that the Arduino architecture is compatible with the Arduino's opensource programming interface; therefore, we can build different scenarios and operate them at once. This low-cost Arduino board has an Atmel SAM3x8E Arm Cortex-M3 central processing unit built on easy-to-use open hardware [43]. It relies on a powerful 84 Mhz and 32-bit ARM-type core

microcontroller. It has more inputs and outputs than other usual Arduino boards, and it is faster and has more analog and communication pins. There are 54 digital input, and output pins, 12 of these pins provide pulse width modulation (PWM) output, 12 analog input pins, and 2 analog output pins. Moreover, the board can store enough data in the internal flash memory, around 512 KB providing more data allocation to operate complex tasks [44].

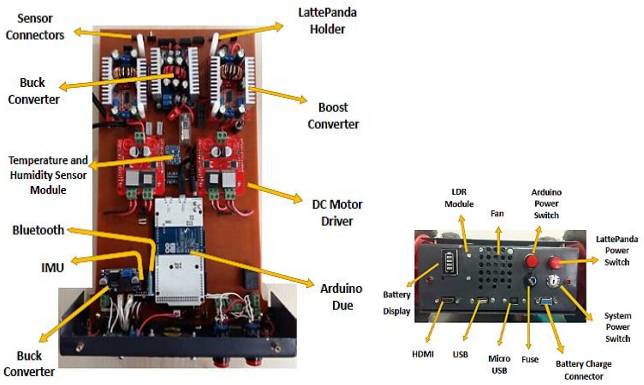

Figure 4. The SMaRt circuit board and its back view.

The developed robot has a wide range of sensor devices for interacting with the physical world. To process the sensors' data, the LattePanda development board [45] is utilized for the SMaRt. The LattePanda is a development board capable of running Windows 10 and Linux. We may connect USB supported devices, such as LIDAR, or a camera, to USB 3.0 and 2.0 ports. It is not only a low-cost regular Windows computer but also has a built-in Arduino that connects actuators and sensors if needed. The LattePanda has plug-and-play headers and general-purpose input/output (GPIO) pins that support standard 5V sensors and actuators, enabling the robot to interact with the working environment. Various information from the environment required is obtained instantly with the HDMI input or the display port, and the data is transferred to the secured digital (SD) card. As shown in Fig. 4, we also put a micro USB at the back side of the SMaRt to reprogram the Arduino card without removing it from the system. The LattePanda, connected to the system through HDMI or USB for motion vision, is an optional card exchanged with other cards such as Raspberry Pi 4 [46] and NVIDIA Nano [47]. The general circuit board and its back views are shown in Fig. 4.

2) Motors and Drivers: The SMaRt is constructed for various purposes, functions, and working environments, so there are several elements to contemplate when selecting a proper actuator. The SMaRt uses four 12V brushed direct current (DC) motors to provide its mobility. For details, refer to [48]. Determining the type of actuator required for convenient functionality is essential. Brushed DC motors have been operated in many fields. They are inexpensive and deliver continuous power and good torque for extended research and education purposes.

The physical size and weight of the actuator itself are also essential to see if it fits in the intended use and if the combined weight of the actuator and the static platform is appropriate. The actuators are chosen as much as lighter, and each weight is 210 grams, and they may not cause the system to fail under the actuator weight. The size of the actuator (37Dx72.5L mm) suits the mounting space on the system properly. It is also crucial that the selected actuator is strong enough to fulfill the robot's working requirements. It provides enough power to move the robot and the robot's load in the operating environment. Its maximum output power and stall torque at 12V is 6W and 45 kg.cm, respectively. The worst-case scenarios are that the robot's load becomes overly heavy and the working condition is challenging to navigate, which are also considered during the actuator selection. The maximum weight of the system is presumed to be 10 kg. The criterion of climbing a 10-degree slope with an acceleration of 0.1 m/s is considered.

The DC motors have a 131.25:1 metal gearbox and an integrated incremental optic encoder that provides a resolution of 64 counts per revolution of the motor shaft. The motors are driven separately by the Sparkfun Monster motor driver modules with a dual output control ability [49]. The modules have 2 VNH2SP30-E H-bridge integrated circuits and require a maximum of 16V, a continuous current draw of 14A, and a maximum PWM frequency 20kHz for each dual motor control performance. The drivers also have automatic shutdown in case of low voltage, over-voltage, overheating, and a current sensing feature.

3) Sensors: This section introduces the sensor selections and their placements. The SMaRt includes ultrasonic sensors (USs), infrared sensors (IRs), a stereo camera, a LIDAR, IMU, a humidity and temperature sensor, and a LDR. There are several factors in choosing convenient sensors for the SMaRt, such as application type, working environment, power consumption, and costs.

The SMaRt has three analog Sharp IRs [50] measuring distances from the obstacles and is used as an on-off switch to avoid obstacles. They are lower-cost sensors and offer faster response times than the US sensors, i.e., 38_10ms. However, infrared sensors have some limitations, like the inability to use them in sunlight, making it difficult for outdoor or dark indoor applications. Three affordable Hc-sr04 digital US sensors [51] installed on the robot are utilized to execute real-time obstacle avoidance. The robot can continually detect surroundings, avoid obstacles, and move toward the desired location. The US sensor, which works with 5V and draws a 15mA current, can measure distances up to 4 meters. However, US sensor measurement accuracy is sensitive to temperature and object shape changes. For example, US performance is ineffective on soft, curved, and thin object surfaces where there is low reflection. This study uses both US and IR sensors to decrease each sensor's sensitivity changing with the working environment.

The ambient temperature, humidity, and air pressure information are obtained from the pressure, temperature, and humidity sensor module connected to the Arduino. The robot's interior temperature is also measured with this sensor. So, the fan on the rear panel is activated based on the internal temperature where cooling is required. In addition, the ambient light intensity is measured through the LDR module on the rear panel. Thus, the environment is illuminated with the LEDs on the front and back of the robot if needed.

Moreover, the SMaRt requires an undersized, lightweight, compatible, and high-quality camera to identify objects, avoid obstacles safely, and find the path without human guidance through a large-scale 3D map of the working environment. The ZED camera [52] allows the SMaRt to provide an extended range of computer vision abilities for education and research purposes. The robot can sense the surroundings in 3D for indoor and outdoor usage up to 20m. It has a high field of view, i.e., 110°(H)x70°(V)x120°(D) at max, and is compatible with

Linux and Windows. However, environmental and lighting conditions can affect camera vision performance; therefore, accurate 3D measurement data is required over short to long ranges.

LIDAR technology can enable obstacle detection, avoidance, and safe navigation through various challenging terrain operations. This study uses a LIDAR designed by SLAMTEC [53]. It determines which obstacles are nearby and how far away they are. Not only do we detect and position objects, but we also identify what they are. We can even use it to predict how objects behave and adjust the SMaRt driving accordingly. However, the LIDAR system is an expensive sensor. It has moving parts, making it easier to break or malfunction and thus more costly to maintain. It also has difficulties in bad weather conditions such as heavy rain, snow, and fog.

For system localization and control purposes, such as inquiring about the current mobile platform position and orientation, an IMU module is also mounted on the system. This sensor adds cost-effective, practical, and ease-of-use solutions to the SMaRt. However, the accuracy of such sensors is affected due to the noise and drifts. It is noted that their performances are sensitive and unstable to changing working conditions.

The reason for installing the sensors mentioned above on the system is to overcome the individual sensor limitations through sensor fusion algorithms if required. Therefore, the students and researchers can build a variety of sensor fusion algorithms. Each sensor can be combined with other sensory data to provide more reliable required data in indoor and outdoor applications related to localization, mapping, path planning, and obstacle avoidance.

4. THE SMaRt SOFTWARE SPECIFICATION

As mentioned in the hardware section, the developed platform has two controllers: the Arduino Due and LattePanda. The main aim of this section is to present the software architectures used to program those control boards. This study uses the Arduino Integrated Development Environment (IDE) to manage the wheel control. The Arduino is used not only for the wheel but also for the IMU, LDR, pressure, temperature and humidity module, Bluetooth module, LEDs, and fan. Any control algorithm, either basic or advanced, can be written in the IDE and uploaded to the Arduino board quickly. The main reason for choosing the Arduino IDE is that it offers userfriendly and free-of-charge software; therefore, students and researchers can build, modify, and enhance their codes freely and operate many different operations ranging from building low-cost scientific instruments to advance robotics.

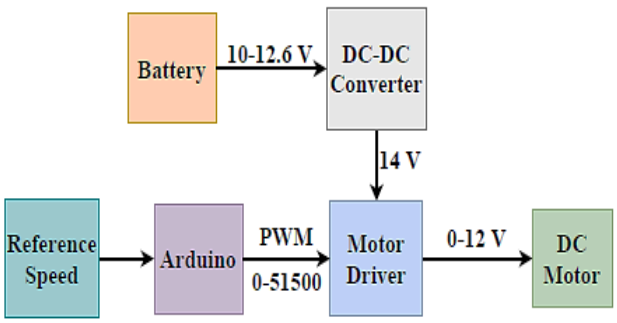

Figure 5. The power management scheme of the SMaRt.

For instance, teachers can quickly build a code to prove physics principles with various robotics applications for educational purposes. At the same time, because of its flexibility, researchers can apply advanced algorithms related to engineering and science fields and exhibit their projects on the SMaRt. One can also share ideas online with Arduino's open community and can improve their programming skills. If any problem occurs in the Arduino, one can easily communicate with the online forums and find answers freely. With advanced integrated sensors such as the camera and

LIDAR, the SMaRt can collect data in real-time to make informed decisions through the LattePanda. They can provide positional information that allows the SMaRt to self-localize and react to change. However, processing such data with any programming language and sending them from the LattePanda to the Arduino to control the wheels is not as easy as it looks. To handle this challenge, we make a serial connection with Arduino and LattePanda through the universal asynchronous receiver transmitter (UART) protocol.

The SMaRt allows the usage of many popular programming languages, such as Python and VB.Net, with its strong controller boards. For example, with its libraries, Python can detect obstacles with the ZED camera through the LattePanda. The instant robot information is transferred to the Arduino board to adjust the robot's positioning. Since LattePanda is compatible with Linux, the ROS environment can also be installed and allow to execution of many applications such as Simultaneous localization and mapping (SLAM) and path planning. Moreover, the developed robot supports MIT App Inventor's applications, allowing one to build fully functional applications for smartphones and tablets to control the robot.

5. THE SMaRt POWER SYSTEM

This section gives an overview of the robot's energy management. We first show how to generate motor power to operate the robot; then, we examine the hardware's energy consumption to uncover the system's required battery power.

5.1. Motor Power Management

This study uses a PWM signal to change the motors' speeds. The motor management scheme is shown in Fig. 5. PWM is an efficient and easy method to control the speed and manage motor power. It drives the motor with the desired speed through a series of ON-OFF pulses and the duty cycle alteration. The SMaRt has four 12V DC motors. Two Sparkfun Monster motor shields are used to manage the control signal of these motors, each with a double output. The PWM signals are sent to the motor drivers through the Arduino card to adjust the desired motor speed. Each of the motors' working ranges is between 0 and 12V, and the motor speed varies linearly with the voltage. The PWM signals typically work with a duty period ranging from 0 to 255 and are obtained from a microprocessor with 8-bit PWM resolution. To raise the motors' control precision, we adjust the PWM resolution to 16 bits, which pushes the maximum PWM value to 65535 from 255. So, the robot will not move with a 0 PWM value given to the driver fed with a 12V constant. When the PWM value of 65535 is assigned, the driver output becomes 12V, and the motor runs with the maximum motor speed.

The continuity of the robot's performance is also essential during the task. The robot needs to maintain its voltage

throughout the operation to obtain the same mechanical power while running. However, as the motors are powered by a 3S lipo battery, not a constant voltage source, and the battery powering the robot is depleted, the required motor voltage applied to the motors will drop over time, degrading the robot's motion performance. Therefore, the lower voltage provides less power and slower motor speeds. Moreover, the battery's voltage values, which have a nominal value of 11.1V, are 12.6V and 10V at full charge and critical level, respectively. So obtaining stable results with varying motor voltages is challenging.

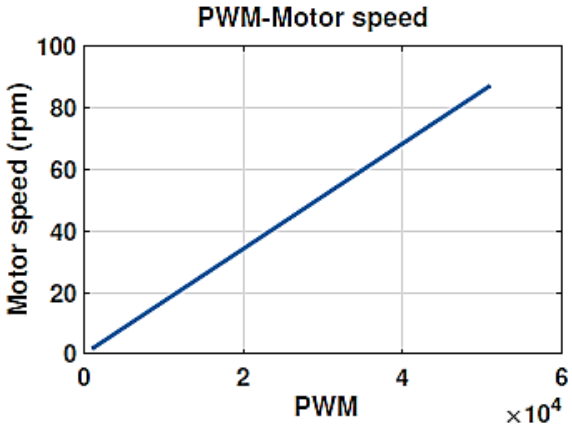

Figure 6. A relationship between the motor speed and PWM value.

DC-DC boost converters are used between the battery and the motor driver to stabilize the voltage applied to the motors, as seen in Fig. 5. The converter outputs are set to deliver a voltage of 14 V as they must be larger than the input. So the driver input remains constant at 14 V even if the battery voltage changes between 12.6 and 10 V. Thus, the maximum speed capability of the motors will not change over time. When the PWM value signaled from Arduino is limited between 0 and 65535, the corresponding applied voltage to the motors will be 0 and 14V, respectively. However, the motors run at a maximum of 12V. So we readjust the maximum PWM value to 51500 to decrease the maximum voltage to 12V. Since the PWM values are important to adjust the motor speed, we present a relationship between the motor speed and the motor PWM values, which is demonstrated in Fig. 6. The results show a straight line relationship between the motor speed and the PWM values, and the maximum speed of 88 rpm is achieved with the value of 51500 at 12V. The motor speed is calculated as follows:

$$w_i = \frac{T w_{max}}{T_{max}} \tag{1}$$

where w_i denotes the i-th instant motor speed, T is a given PWM value to adjust the speed, w_{max} means a maximum motor speed capacity, and T_{max} represents a maximum PWM value. From the experimental results presented in Fig. 7, it is observed that the measured motor speed matches the calculated motor speed. Moreover, it is seen that the relationship between the motor speed and period has an exponential decay characteristic, and the motor speed reaches its maximum speed at a period of 0.2 ms. As seen in Fig. 7, the motor speed falls exponentially over time before reaching a plateau at 1 ms.

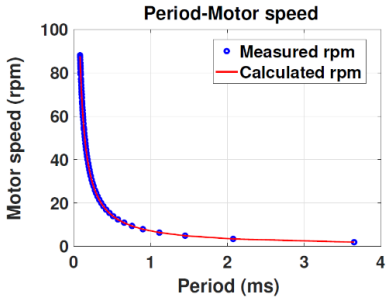

Figure 7. A relationship between the motor speed and motor period.

5.2. System Power Management

This section introduces the power management and power requirements of the SMaRt. The robot power supply impacts the robot's performance, and any failure occurring in the power supply may prevent the completion of the task successfully. Therefore, it is necessary to calculate the required power to move the robot with a battery in unstructured and structured environments. The robot's power consumption has been calculated by considering the amount of each device's power consumption. When the system is activated without the motors, LattePanda, camera, IR, and US sensors, the electronic circuits draw a current of 0.23A. This provides the robot with approximately 26 hours of operation when the application is executed on the Arduino board with electronic circuits. When the robot is operated manually with the PWM value of 26000 in the absence of the LattePanda, camera, and object detection sensors in the laboratory environment where it is a flat floor without slope, it draws an instantaneous current of 1.05A. The robot's power consumption varies depending on the task's difficulty, changing the battery's service life. Moreover, we calculate the robot weight for two mounted batteries with 3S 6Ah during the design procedure, so one can install an extra battery to double the robot's operation time if required.

6. EXPERIMENTS AND RESULTS

This section presents the performances of the SMaRt system and its components. The experimental results are introduced in three parts. The first part of the experiments is conducted to show the IR and US sensors' performances when they are operated in indoor and outdoor environments. Then, the second part of the experiments is realized to reveal the basic functionality of the motor control performances. The robot's suitability for computer vision is examined at the end of this section.

6.1. Performance results of the IR and US sensors

The performance of the IR and US proximity sensors are demonstrated in Figs. 8 and 9 for indoor working environments with bright and dark light conditions. Fig. 8 shows the performance results of the percentage measurement error for each surface color of the obstacle using the IR and US sensors. Fig. 8 demonstrates that the IR sensor has better overall accuracy than the US sensor despite changing surface colors. The results show that the US sensor outperforms the IR sensor when measuring the obstacle distance in close proximity. However, the measurement error increases when the distance between the obstacle and the robot is more than 300 mm. The minimum error for the IR sensor is achieved with the red color obstacle surface. However, it is noted that the percentage error

for the IR sensor is higher for the transparent surface obstacle, as shown in Fig. 8.

We also examine the impact of the changing environmental condition on the sensors' performances. Fig. 9 shows the sensors' performances in the dark indoor environment. The IR sensor outperforms the US sensor in case of measuring the obstacles in close proximity. The US sensor has a better performance when it is operated in a dark indoor working environment. Compared to long-distance measurement, the US sensor performs poorly when the obstacle is brought to a 300 mm distance. The IR sensor can detect an obstacle in the range of 300 to 1200 mm.

The sensors' performances are also examined in an outdoor environment, and the results are shown in Fig. 10. It is seen that the US sensor outperforms the IR sensor. The IR sensors can measure the obstacle distance at only 300 mm with almost 50 percent measurement error. However, the US sensor can measure distances ranging from 300 mm to 1500 mm except for the transparent surface at 300 mm.

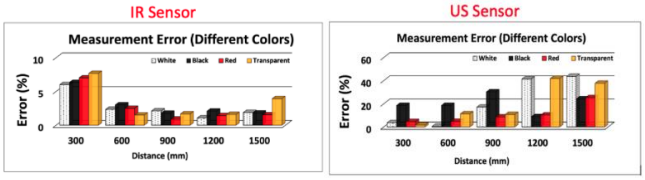

Figure 8. IR and US sensors' measurement errors in percentage with different surface colors in a bright indoor environment.

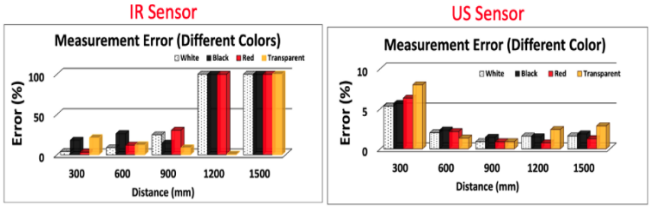

Figure 9. IR and US sensors measurement errors with different surface colors in a dark indoor environment.

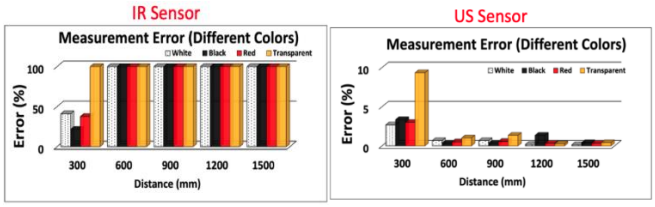

Figure 10. IR and US sensors measurement errors with different surface colors in an outdoor working environment.

6.2. Performance results of the motor speed control

The experiments are performed at different motor speed levels for a closed loop case. The motor is assigned to the PWM generator, and the error is observed using the encoder. For the closed-loop case, we choose a PID controller to handle the motor speed error and show the closed-loop controller performance over the non-controller case. The motor control performances are demonstrated in Figs. 11-13. Fig. 11 shows the motor performance without a controller. From Fig. 11, it is seen that the motor speed does not converge to reference motor speed over time at different speeds. The motor control performance in tracking the reference is low at a slow pace. For the closed-loop scheme, we choose PID controller parameters after several trials to make the motor movement more smooth. Figs. 12 and 13 show the closed-loop motor performances with different controller parameters. The results shown in Fig. 12 is obtained from choosing kp = 0:1, kd = 0:1, and ki = 0:01. Keeping the derivative and integral control parameters the same and decreasing the proportional control parameter to 0.05, we have a reduced steady-state error, thus making the system performance more stable, as shown in Fig. 13. In addition, considering different environmental conditions, it may be necessary to change the parameters since dynamic equations are not used.

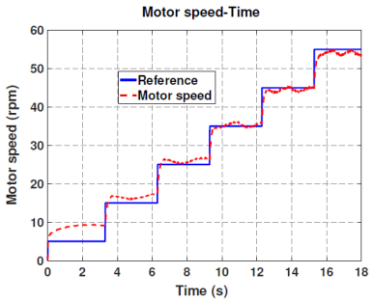

Figure 11. The motor control performances at different speed references without a controller.

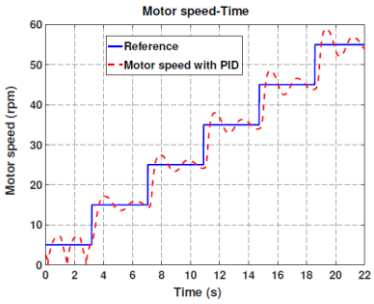

Figure 12. The motor control performances at different speed references with PID controller. The parameter coefficients are kp = 0:1, kd = 0:1, and ki = 0:01.

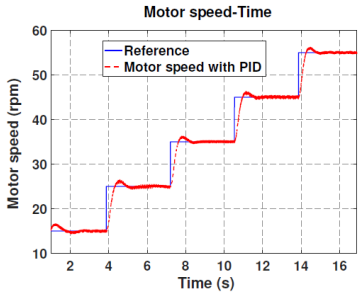

Figure 13. The motor control performances at different speed references. The parameter coefficients are kp = 0:05, kd = 0:1, and ki = 0:01.

6.3. Performance results of the system motion

This section shows a simple motion describing how the robot approaches a traffic light with a PID controller. We show the motor speed control performance during the operation and the applicability of the SMaRt's camera. We also designed an Android app through the MIT App Inverter to set the desired robot position, speed, and PID controller gains. We propose a camera-based algorithm for locating the traffic light and detecting the light colour during the performance.

The algorithm's first part explores the You only look once (YOLO) architecture [54] for real-time traffic light detection. The SMaRt first need to locate the traffic light correctly and leave out the other objects around the working environment. So we can eliminate things lighting the green and red lights except for the traffic light. The YOLOv4 algorithm is used to predict

the traffic light probability and simultaneously bound it with a box.

After detecting the traffic light location, the instant camera images are loaded to identify green and red traffic lights through classic image processing to get the RGB image values as a second part of the algorithm. The images in RGB colour space are then converted to hue, saturation, and value (HSV) colour space, and a mask is applied to detect the candidate colours. The light candidates are determined based on colour intensity on the obtained HSV colour space image. The camera images during the performance and the results after applying the masks are shown in Fig. 14.

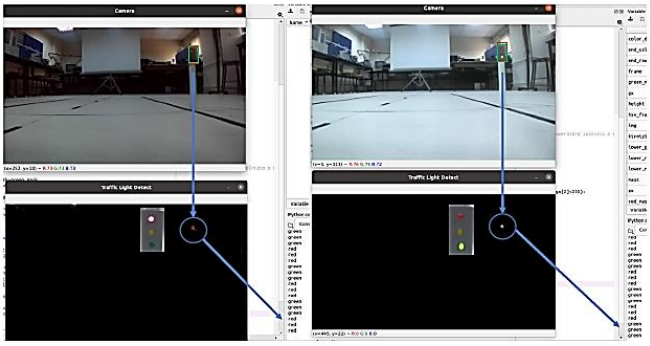

(a) (b)

Figure 14. Traffic light detection and control (a) sensing the red traffic light and (b) sensing the green traffic light.

During the performance, we set the system parameters such as desired robot position, speed, and controller parameters through the Android application, designed for convenient usage. The proposed application with MIT App Inventor consists of three components: the main screen, the manual control screen, and the automatic control screen. The main screen is where the actions of the control preference selection, such as manual control and automatic control and the Bluetooth connection between the mobile robot and Android phone occur.

The manual control screen is employed to adjust the desired robot movement and speed by hand when the robot is operated manually for calibration or manual positioning purposes. In the case of the need for automatic motion control, the desired robot position, speed data, and control parameters are inserted into the mobile robot processor through the automatic control screen. The screen views of the mobile app are shown in Fig. 15. As shown in Fig. 15b, the user can easily insert the desired parameters and operate the robot through the app screen. For details regarding the interactive Android application, the reader is referred to [55].

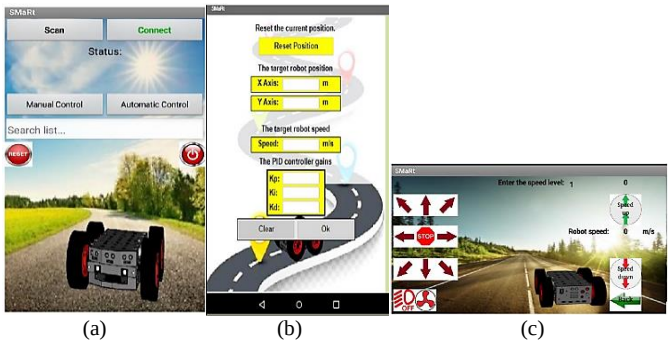

(a) (b) (c)

Figure 15. The SMaRt's mobile application screen views are designed with the MIT app inverter: (a) the main screen view,(b) the automatic control screen view, and (c) the manual screen view.

The predefined path is shown in Fig. 16. The motion planning scenario has three phases. The first is that the robot approaches the traffic light with a green light. Then, the robot continues to move toward the traffic light. The robot decreases speed and stops when the camera detects the red light. In the third phase, the robot starts to move forward when the red light turns green.

The motors' speed performances during the motion planning are given in Fig. 17. The robot moves through the path at 25 rpm for four seconds of motion. When it faces the traffic light at the red light, the motors stop for five seconds. When the traffic light turns green again, the motors start working at 25 rpm. After several trials, the control design parameters are chosen, and the results show that the reference speed tracking is achieved with the developed PID controller. The results reveal that each motor speed of the SMaRt converges to the desired speed during the motion performance. In addition, it may be difficult to detect the traffic light in dark weather conditions. Moreover, since the connection is provided via Bluetooth, the user must be closer than ten meters to the robot.

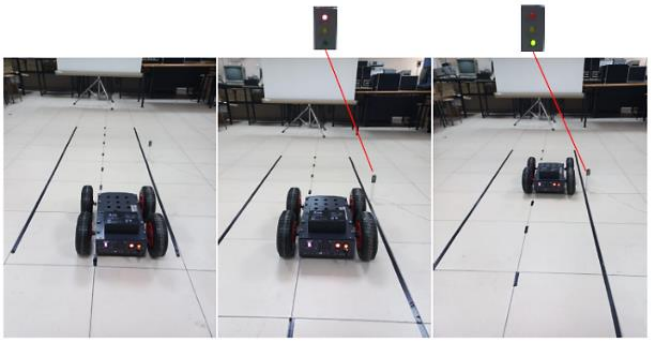

(a) (b) (c)

Figure 16. The SMaRt is on a pre-defined path: (a) moving through the path, (b) stopping at the red light, (c) moving at the green light and passing the traffic light.

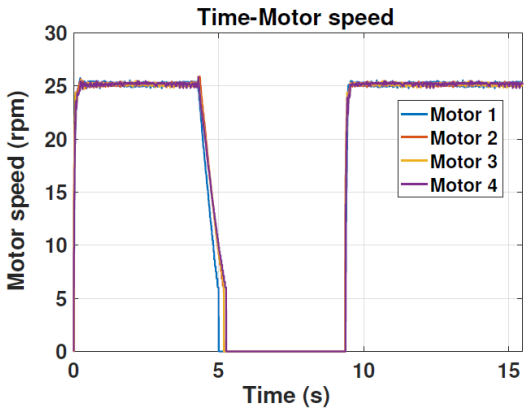

Figure 17. The SMaRt's motor speed performance with the PID controller during the motion planning.

7. CONCLUSION

This article presents SMaRt's features and capabilities. The SMaRt is operated in many educational fields, especially in engineering, with its advantages, such as reprogramming, remote control, and modular design. Due to its durable, symmetric, and shock-reducing spring structure, the robot works in the military, service, and health fields. Any required information about the working environment is obtained from the sensors so that the robot can complete the operation

smoothly. The developed robot allows the realization of advanced applications such as path-planning, mapping, and real-time image processing. We can easily reprogram the robot without disassembling any parts because the Arduino's programming port for the motor control and LattePanda's USB and HDMI ports for image processing or other related algorithms are conveniently placed on the robot. The battery charging slot is also located at the back, so it is charged without dismantling the platform. To increase the robot's mobility, the SMaRt allows quickly exchanging the wheels type for the Mechanum and integrating the pallet system if required. The robot circuit allows an extra battery connection in parallel, which provides a longer robot performance. For future work, we will generate the robot's kinematic and dynamic models and apply advanced control algorithms for the system positioning. Moreover, path-planning algorithms will be performed so the robot can work autonomously in real time.

ACKNOWLEDGEMENT

This study is supported by Fırat University Scientific Research Projects Unit (FUBAP) with the project number TEKF.19.07. So the authors would like to express their gratitude to the **FUBAP** for their financial support.

REFERENCES

[1] Calo R. *The case for a federal robotics commission*. Available at SSRN 2529151, 2014.

[2] Felicia A, Sharif S. A review on educational robotics as assistive tools for learning mathematics and science. Int. J. *Comput. Sci. Trends Technol, vol. 2*, no. 2, pp. 62–84, 2014.

[3] Khine, M. S., Khine, M. S., & Ohmer. *Robotics in STEM* Education. Springer, 2017.

[4] Merdan, M, Lepuschitz, W, Koppensteiner, G, & Balogh R. Balogh, *Robotics in education*: Research and practices for robotics in STEM education, vol. 457. Springer, 2016.

[5] Eguchi, A. Robocup junior for promoting stem education, 21st-century skills, and technological advancement through robotics competition. *Robotics and Autonomous Systems, vol. 75*, pp. 692–699, 2016.

[6] Curto B, Moreno V. Robotics in education. *Journal of Intelligent & Robotic Systems, vol. 81*, no. 1, p. 3, 2016.

[7] Lindsay S, and Hounsell KG. Adapting a robotics program to enhance participation and interest in stem among children with disabilities: a pilot study. Disability and Rehabilitation: *Assistive Technology, vol. 12*, no. 7, pp. 694–704, 2017.

[8] Rivera JH. Science-based laboratory comprehension: an examination of effective practices within traditional, online and blended learning environments. Open Learning: *The Journal of Open, Distance and e-Learning, vol. 31*, no. 3, pp. 209–218, 2016.

[9] Felder RM, Soloman BA et al. *Learning styles and strategies*. 2000

[10] Nguyen, K. A., DeMonbrun, R. M., Borrego, M. J., Prince, M. J., Husman, J., Finelli, C. J., ... & Waters, C. The variation of nontraditional teaching methods across 17 undergraduate engineering classrooms. in 2017 ASEE Annual Conference & Exposition, 2017.

[11] Hernandez-de-Menendez, M., Escobar D´ıaz, C., & Morales-Menendez, R. Technologies for the future of learning: state of the art. International *Journal on Interactive Design and Manufacturing (IJIDeM), vol. 14*, no. 2, pp. 683–695, 2020.

[12] Spolaor, N., & Benitti, F. B. V. Robotics applications grounded in learning theories on tertiary education: A systematic review. *Computers & Education, vol. 112*, pp. 97–107, 2017.

[13] Giang, C., Piatti, A., & Mondada, F. Heuristics for the development and evaluation of educational robotics systems. *IEEE Transactions on Education, vol. 62*, no. 4, pp. 278–287, 2019.

[14] Ceccarelli M. Robotic teachers' assistants. *IEEE Robotics & Automation Magazine, vol. 10*, no. 3, pp. 37–45, 2003.

[15] Piepmeier, J. A., Bishop, B. E., & Knowles, K. A. Modern robotics engineering instruction. *IEEE Robotics & Automation Magazine, vol. 10, no. 2*, pp. 33–37, 2003.

[16] Robinette M.F, Manseur R. Robot-draw, an internet-based visualization tool for robotics education. *IEEE Transactions on Education, vol. 44*, no. 1, pp. 29–34, 2001.

[17] Nagai K. Learning while doing: practical robotics education. *IEEE Robotics & Automation Magazine, vol. 8*, no. 2, pp. 39–43, 2001.

[18] Wu, M., She, J. H., Zeng, G. X., & Ohyama, Y. Internet-based teaching and experiment system for control engineering course. *IEEE Transactions on Industrial Electronics, vol. 55*, no. 6, pp. 2386–2396, 2008.

[19] Gardun˜o-Aparicio, M., Rodr´ıguez-Res´endiz, J., Macias-Bobadilla, G., & Thenozhi, S. A multidisciplinary industrial robot approach for teaching mechatronics-related courses. *IEEE Transactions on Education, vol. 61*, no. 1, pp. 55–62, 2017.

[20] Nao the humanoid and programmable robot. [Online]. Website https://www.softbankrobotics.com/emea/en/nao

[21] Giovannangeli C, and Gaussier P. Interactive teaching for visionbased mobile robots: A sensory-motor approach. *IEEE Transactions on Systems, Man, and Cybernetics-Part A: Systems and Humans, vol. 40*, no. 1, pp. 13–28, 2009.

[22] Jojoa, E. M. J., Bravo, E. C., & Cortes, E.B.B. Tool for experimenting with concepts of mobile robotics as applied to children's education. *IEEE Transactions on Education, vol. 53*, DOI 10.1109/TE.2009.2024689, no. 1, pp. 88–95, 2010.

[23] Arvin, F., Espinosa, J., Bird, B., West, A., Watson, S., & Lennox, B. Mona: an affordable open-source mobile robot for education and research. *Journal of Intelligent & Robotic Systems, vol. 94*, no. 3, pp. 761–775, 2019.

[24] Maxwell B.A, and Meeden L.A. Integrating robotics research with undergraduate education. *IEEE Intelligent systems and their applications, vol. 15*, no. 6, pp. 22–27, 2000.

[25] Mondada, F., Bonani, M., Raemy, X., Pugh, J., Cianci, C., Klaptocz, A., ... & Martinoli, A. The epuck, a robot designed for education in engineering. in Proc. of the 9th conference on autonomous robot systems and competitions, vol. 1, no. CONF, pp. 59–65. IPCB: Instituto Polit´ecnico de Castelo Branco, 2009.

[26] Cianci, C. M., Raemy, X., Pugh, J., & Martinoli, A. Communication in a swarm of miniature robots: The e-puck as an educational tool for swarm robotics. in International Workshop on Swarm Robotics, pp. 103–115. Springer, 2006.

[27] Francesca, G., Brambilla, M., Brutschy, A., Trianni, V., & Birattari, M. Automode: A novel approach to the automatic design of control software for robot swarms. *Swarm Intelligence, vol. 8*, no. 2, pp. 89–112, 2014.

[28] Prieto, A., Becerra, J. A., Bellas, F., & Duro, R. J. Open-ended evolution as a means to self-organize heterogeneous multi-robot systems in real-time. *Robotics and Autonomous Systems, vol. 58*, no. 12, pp. 1282–1291, 2010.

[29] Greenwald L, Kopena J. Mobile robot labs. *IEEE Robotics & Automation Magazine, vol. 10*, no. 2, pp. 25–32, 2003.

[30] G´omez-de-Gabriel, J. M., Mandow, A., Fernandez-Lozano, J., & Garcia-Cerezo, A. Mobile robot lab project to introduce engineering.

[31] Scribbler 3 (s3) robot. [Online]. Website https://www.parallax.com/product/scribbler-3-s3-robot students to fault diagnosis in mechatronic systems," *IEEE Transactions on Education, vol. 58*, no. 3, pp. 187–193, 2014. [accessed 7 May 2023].

[32] Calvo, I., Cabanes, I., Quesada, J., & Barambones, O. A multidisciplinary pbl approach for teaching industrial informatics and robotics in engineering. *IEEE Transactions on Education, vol. 61*, no. 1, pp. 21–28, 2017.

[33] Do Y. Self-selective multi-objective robot vision projects for students of different capabilities. *Mechatronics, vol. 23*, no. 8, pp. 974–986, 2013.

[34] Quanser qbot 3. [Online]. Website https://www.quanser.com/products/qbot-3/ [accessed 12 May 2023].

[35] Pioneer 3-dx robot. [Online].Website https://www.generationrobots.com/media/Pioneer3DX-P3DX-RevA.pdf [accessed 12 May 2023].

[36] Turtlebot 2 robot. [Online].Website https://clearpathrobotics.com/turtlebot-2-open-source-robot [accessed 12 May 2023].

[37] Gritti, A. P., Tarabini, O., Guzzi, J., Di Caro, G. A., Caglioti, V., Gambardella, L. M., & Giusti, A. Kinect-based people detection and tracking from small-footprint ground robots. in International Conference on Intelligent Robots and Systems (IROS), pp. 4096–4103, 2014.

[38] Wu, K., Ranasinghe, R., & Dissanayake, G. Active recognition and pose estimation of household objects in clutter. in International Conference on Robotics and Automation (ICRA), pp. 4230–4237. IEEE, 2015.

[39] Barber, R., Rodriguez-Conejo, M. A., Melendez, J., & Garrido, S. Design of an infrared imaging system for robotic inspection of gas leaks in industrial environments. *International Journal of Advanced Robotic Systems, vol. 12*, no. 3, p. 23, 2015.

[40] Turtlebot 3 robot. [Online].Website https://emanual.robotis.com/docs/en/platform/turtlebot3/overview [accessed 15 May 2023].

[41] Amsters R. and Slaets P. Turtlebot 3 as a robotics education platform. in International Conference on Robotics in Education (RiE), pp. 170– 181. Springer, 2019.

[42] Turtlebot 4 robot. [Online]. Website https://clearpathrobotics.com/turtlebot-4 [accessed 15 May 2023].

[43] Microcontroller. [Online]. Website https: //ww1.microchip. com/downloads/en/devicedoc/ atmel-11057-32-bit- cortex-m3-micro controller-sam3x-sam3a datasheet.pdf [accessed 15 May 2023].

[44] Arduino due. [Online]. Website https://store.arduino.cc/products/arduino-due [accessed 15 May 2023].

[45] Lattepanda. [Online]. Website https://www.lattepanda.com [accessed 17 May 2023].

[46] Raspberry pi 4. [Online].Website https://www.raspberrypi.com/products/raspberry-pi-4-model-b [accessed 17May 2023].

[47] Nvidia jetson nano developer kit. [Online].Website https://developer.nvidia.com/embedded/jetson-nano-developer- kit [accessed 17 May 2023].

[48] Dc motor. [Online]. Website https://www.pololu.com/product/4756/specs [accessed 17 May 2023].

[49] Sparkfun monster moto shield. [Online]. Website https://www.sparkfun.com/products/retired/10182 [accessed 17 May 2023].

[50] Sharp infrared distance measuring sensor. [Online]. Website https: //www.sparkfun.com/datasheets/Sensors/ In- frared/gp2y0a02yk e.pdf [accessed 17 May 2023].

[51] Ultrasonic distance sensor - hc-sr04. [Online]. Website https: //www.sparkfun.com/products/15569 [accessed 17 May 2023].

[52] Zed 1 stereo camera. [Online]. Website https://www.stereolabs.com/zed-1 [accessed 17 May 2023].

[53] Slamtec rplidar-a3 laser range scanner. [Online]. Website https: //www.slamtec.com/en/Lidar/A3 [accessed 17 May 2023].

[54] Redmon, J., Divvala, S., Girshick, R., & Farhadi, A. You only look once: Unified, real-time object detection. In Proceedings of the IEEE conference on computer vision and pattern recognition, pp. 779–788, 2016.

[55] Top, A., & Go¨kbulut, M. Android application design with mit app inventor for bluetooth based mobile robot control. *Wireless Personal Communications*, pp. 1–27, 2022.

BIOGRAPHIES

Ahmet Top received the B.Sc. , M. Sc. and PhD degrees in electric and electronic engineering from the Fırat University, Elaziğ, Turkey, in 2011, 2016 and 2023, respectively. He is currently Research Assistant and working toward the Ph. D. degree at Department of Electrical and Electronics Engineering, Technology Faculty, Firat University. His current research interests include control systems and robotic.

Gökhan Güngör In 2011,graduating with a third degree of the department, obtained his Bachelor of Machine Engineering from the University of Firat, Elazig, Turkiye. He has completed his M. Tech and Ph.D. in Machine and Mechatronic Engineering at University Of Waterloo in 2014 and 2020 respectively. He is currently working at the Karabük University as a assistant professor of the Department of Mechatronic Engineering. İmage prosessing, robotic, artificial intellegent and control theory are his research areas.

Muammer Gökbulut received the B.Sc. in electric education from Gazi University in 1980 and the M.Sc. degree in electric education from Gazi University, Ankara, Turkey, in 1989, and the PhD. degree in electronic engineering from Erciyes University, He is a full Professor at Department of Electrical and Electronics Engineering, Technology Faculty, Firat University, Elazığ, Turkey. His current research interests include Neural network and Adaptive control systems.